Microchemical Journal 138 (2018) 296–302

Contents lists available at ScienceDirect

Microchemical Journal

journal homepage: www.elsevier.com/locate/microc

Emitter/receiver piezoelectric films coupled to flow-batch analyzer for acoustic determination of free glycerol in biodiesel without chemicals/external pretreatment

Gabriel M. Eggly [a], Matías Blackhall [a], Adriano de Araújo Gomes [b], Rodrigo Santos [a], Mário César Ugulino de Araújo [c], Marcelo F. Pistonesi [d,*]

[a] Dep. Ingeniería Eléctrica y de Computadoras, Universidad Nacional del Sur, IIIE-CONICET, Av. Alem 1253 (B8000CPB), Bahía Blanca, Buenos Aires, Argentina
[b] Departamento de Química Inorgânica – DQI, Instituto de Química – IQ, Universidade Federal do Rio Grande do Sul, Instituto de Química-UFRGS. Av. Bento Gonçalves 9500 Agronomia 91501970 - Porto Alegre, RS - Brasil
[c] Universidade Federal da Paraíba, Dep. de Química, Laboratório de Automação e Instrumentação em Química Analítica/Quimiometría (LAQA), Caixa Postal 5093, 58051-970 João Pessoa, PB, Brazil
[d] Dep. de Química, Universidad Nacional del Sur, INQUISUR, Av. Alem 1253 (B8000CPB), Bahía Blanca, Buenos Aires, Argentina

ARTICLE INFO

Article history:
Received 13 October 2017
Received in revised form 12 January 2018
Accepted 17 January 2018
Available online xxxx

Keywords:
Flow-batch
Piezoelectrics
PLS models
Biodiesel
Glycerol

ABSTRACT

This paper describes for the first time the use of emitter and receiver piezoelectric films coupled one in front of the other into a flow-batch analyzer for acoustic determination of free glycerol in biodiesel without chemicals/external pretreatment. Online extraction of free glycerol from biodiesel was carried out into aqueous solution without chemicals/external pretreatment. While the emitter piezoelectric is activated to sonicate the solution, the receiver piezoelectric translates the acoustic signal received into an electrical signal, which is measured and recorded by a digital oscilloscope. Multivariate calibration models were built for prediction of free glycerol concentration. In this sense, results of partial least square regression (PLS), the interval PLS (iPLS) and PLS coupled with the Successive Projections Algorithm for interval selection (iSPA-PLS) were compared. The proposed low-cost flow-batch analyzer exhibited good performance, satisfactory detection limit (0.12 mg kg^{-1}) and a linear response from 72 to 372 mg kg^{-1} of free glycerol in biodiesel. The procedure was successfully applied to the analysis of biodiesel samples, and the results agreed with the reference method (ASTM D6584-07) at 95% confidence level.

1. Introduction

Biodiesel is a great substitute for petroleum diesel that can be used on any unmodified diesel engine. It has important characteristics that make it attractive since it is a renewable, non-toxic, biodegradable and ecofriendly fuel [1]. Blends of biodiesel and diesel are the most commonly products distributed for use in the retail biofuel marketplace. However, the biodiesel manufacturing process generates approximately 10% (w/w) of glycerol as the sub-product main [2–3]. Since glycerol is slightly soluble in esters (biodiesel), glycerol present in biodiesel causes negative effects on the diesel engine, such as clogging fuel filters, fouling fuel injectors, and forming a deposit on the bottom of fuel storage tanks [4–6]. In order to minimize the problems caused by glycerol, sustain production of biofuels, and provide quality control criteria to this developing industry, ASTM and other regulatory organizations have established limits of 0.02% (w/w) for free glycerol [7]. Therefore, accurate and sensitive methods are needed for the determination of free and total glycerol in biodiesel. Several methods for determining free glycerol content in biodiesel have been developed based on chromatographic [8–9], amperometric [10], and spectrophotometric techniques [11–13]. Also, sonoluminescent flow-batch method to determine free glycerol in biodiesel was proposed by Diniz et al. [14]. In this work, water was used to generate water-cavitation sonoluminescence signals, which were modulated by the quenching effect associated with the amount of free glycerol. The method requires the use of a photomultiplier tube (PMT) as detector that needs a stabilized high voltage power supply to achieve a reasonable sensitivity and noise immunity. The generation of the water-cavitation signal was achieved using a ceramic piezoelectric device. The use of piezoelectric technology has been increased significantly in recent years. It can be used both as sensor or actuator based on its capability as a transducer device [15–17]. Like every transducer, it converts one form of energy into another (in this case, mechanical into electrical and vice-versa). It produces voltage or charge proportional in both amplitude and frequency to an applied dynamic strain [18]. In 1969, Kawai found very high piezo-activity in the polarized fluoropolymer, polyvinylidene fluoride (PVDF) [19]. New copolymers of PVDF, developed over the last few years, have expanded the applications of

* Corresponding author.
E-mail address: mpistone@criba.edu.ar (M.F. Pistonesi).

https://doi.org/10.1016/j.microc.2018.01.027
0026-265X/

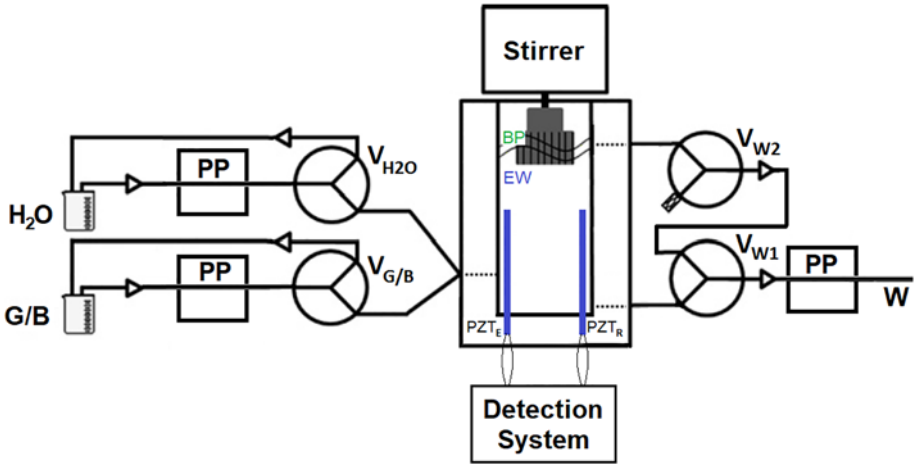

Fig. 1. Schematic diagram of the flow-batch analyzer. Three-way solenoid valves (V), lab-made peristaltic pump (PP), biodiesel phase (BP), extractive water (EW), emitter (PZT_E) and receiver (PZT_R) piezoelectric films, waste (W), glycerol standard solution or biodiesel sample (G/B).

piezoelectric polymer sensors [20–21]. One major advantage of piezoelectric film over piezoelectric ceramic is its low acoustic impedance, which is closer to that of water, human tissue and other organic materials [22]. Although piezoelectric film has low density and excellent sensitivity, and it is mechanically tough. Additionally, when extruded into thin film, piezoelectric polymers can be directly attached to a structure without disturbing its mechanical motion [23]. The demand of these sensors has been propelled by the growth in the use of microcontrollers. Diverse applications in the field of chemistry could be found in the literature [24–26].

This paper describes for the first time the use of emitter (PZT_E) and receiver (PZT_R) piezoelectric films coupled one in front of the other into a flow-batch analyzer for acoustic determination of free glycerol in biodiesel without chemicals/external pretreatment. While PZT_E is activated to sonicate, PZT_R translates the acoustic signal received into an electrical signal, which is measured by the data acquisition system.

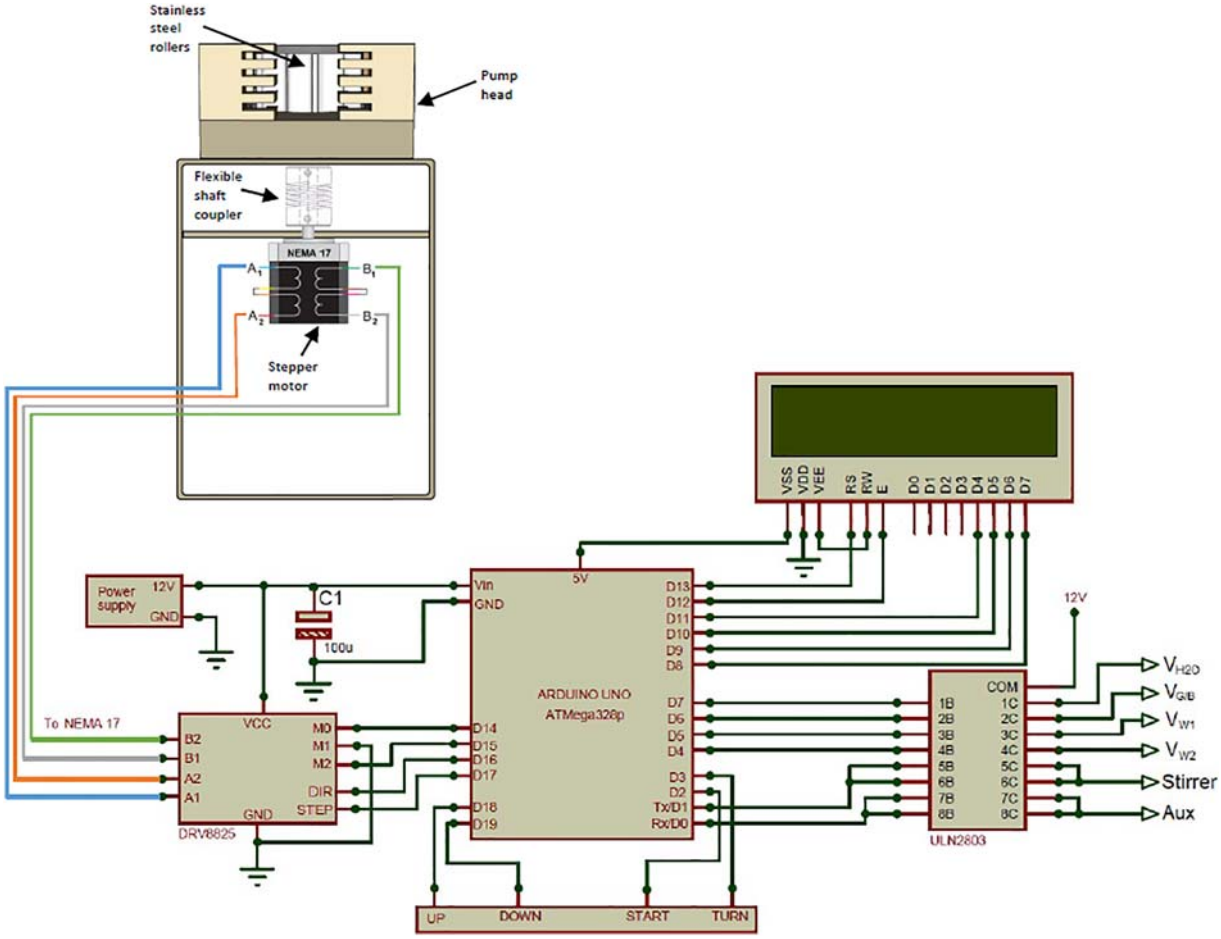

Fig. 2. Lab-made peristaltic pump coupled to the schematic circuit of the flow-batch analyzer controller unit.

Table 1
Flow-batch procedure.

Steps	Events	Time (s)	Pump setup (RPM)	Volume (mL)	Pump tube (mm i.d.)
1	Water (V_{H2O})	15.2	20	1.600	2.06
2	Biodiesel ($V_{G/B}$)	30.7	10	0.455	1.29
3	Stirring[a]	240	0	–	–
4	Wait[a]	5	0	–	–
5	Waste (V_{W2})	10	20	–	2.06
6	Detection	5	0	–	–
7	Waste (V_{W1})[b]	20	20	–	2.06
8	Water (V_{H2O})[b]	15.2	20	1.600	2.06
9	Stirring[b]	30	0	–	–
10	Waste (V_{W1})[b]	20	20	–	2.06

[a] Extraction time.
[b] Cleaning.

The multivariate calibration models were built relating free glycerol concentration and the recorded multivariate signal in PZT_R. For comparison purpose, partial least square regression (PLS), the interval PLS, (iPLS) and PLS coupled with the Successive Projections Algorithm for interval selection (iSPA-PLS) were used [27–28].

2. Experimental

2.1. Samples and solutions

Stock solution was prepared by dissolving 83.9 mg of glycerol (99.5%, Mallinckrodt) in 250 ml of water. The samples of biodiesel were obtained from the Petrobras refinery located in the city of Bahia Blanca, Argentina. Distilled-deionized water (18 MΩ/cm) was used exclusively throughout the entire study.

2.2. Flow-batch analyzer

A schematic diagram of the flow-batch analyzer (FBA) used for acoustic determination of free glycerol in biodiesel is shown in Fig. 1. FBA consists of four NResearch model 161 T031 three-way solenoid valves ($V_{G/B}$, V_{H2O}, V_{W1} and V_{W2}), polyethylene tubing connectors with 0.8 mm i.d., Tygon® pumping tubes (1.29 and 2.06 mm i.d.), a PTFE flow-batch chamber (FBC) with 2.5 mL of total volume, an acoustic detection system based on emitter/receiver piezoelectric films, lab-made peristaltic pump and a flow-batch controller unit.

FBC has a fixed stirrer on the top, which is turned by a DC motor (MDN3, 9VDC). Two flexible piezoelectric films (MEAS-SPEC LDT1-028 K) attached to the walls of FBC fulfill the function of emitter and receiver of an ultrasound wave. The acoustic impedance of piezoelectric film is only 2.6 times that of water [22]. This permits more efficient transduction of acoustic signals in water.

A digital oscilloscope OWON DS7072 carried out the recording of the received electrical signal that was processed later in a personal computer.

As indicated in Fig. 1, the piezoelectric films were located at the inferior laterals of FBC, one in front of the other. Thus, the acoustic waves generated by emitter piezoelectric (PZT_E) travel through the solution and is then captured by the receiver piezoelectric (PZT_R).

The lab-made peristaltic pump (Fig. 2) was constructed with a stepper motor and a pump head of four channels and 10 stainless steel rollers to achieve a precise, smooth and low pulse flow. Propelling fluids may require high pressure and therefore high torque generated by the stepper motor. For this reason, it was used a Nema17 high torque bipolar stepper motor (17HS6002) to drive the pump. The shaft of the Nema17 and the peristaltic pump head were coupled with a 5 mm aluminum flexible shaft coupler. To drive the Nema 17, the DRV8825 (Pololu) high current stepper motor carrier was used.

The FBA controller unit (Fig. 2) has a Human-Machine-Interface (HMI) that allows users to configure and display the FBA parameters. It consists of a LCD display (HD44780), two buttons for start/stop and for change the direction of rotation (turn), and a rotary encoder switch (up and down) to modify the parameters. The driving circuit for activating the solenoid valves and the stirrer was implemented with the integrated circuit ULN2803 (Texas Instruments). It consists of an array of eight Darlington transistors specially designed to handle inductive loads up to 0.5 A per driver. The automation of the system was done with an ATMega328 microcontroller (Arduino UNO open-hardware kit). This 8-bit MCU provides the necessary on-chip peripherals for this purpose at a low cost. An 8-bit timer was used to implement a time-base for the whole system. Digital outputs ports were used for interfacing the peripherals components (DRV8825, ULN2803, LCD, etc). A Pulse Width Modulation (PWM) signal controls the speed of the stirrer.

2.3. FBA procedure

Initially, working solutions for each channel are pumped and re-circulated to their respective reservoirs and solenoid valves V_{H2O} and $V_{G/B}$ are simultaneously switched ON for 5 s, filling the channels located between all valves and FBC. After that, the waste valve (V_{W1}) is switched

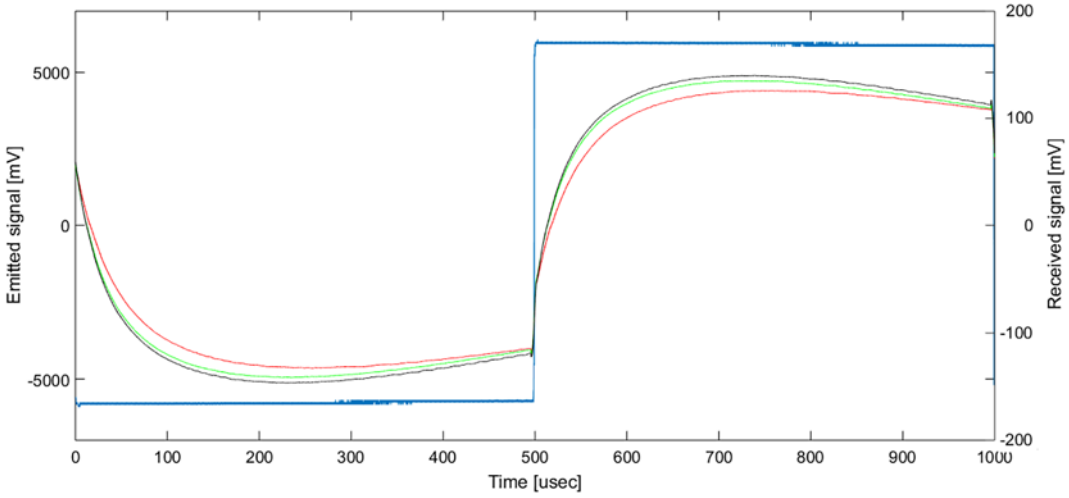

Fig. 3. Curves from the emitted signal (blue line) and the pre-processed received signals of 18.736 (red line), 84.312 (green line) and 93.680 (black line) mg/L glycerol in water solution. (For interpretation of the references to colour in this figure legend, the reader is referred to the web version of this article.)

ON for 20 s, FBC is emptied and the wash cycle is carried out as described below. The filling of the channels between valves and FBC should be always performed.

For acoustic determination of free glycerol in biodiesel without chemicals/external pretreatment, FBA was operated using the optimized experimental conditions presented in Table 1.

The online preparation of calibration solutions (18–93 mg/L glycerol, being equivalent to 72–372 mg kg^{-1} free glycerol in biodiesel) is performed in the FBC by using different volumetric ratio of the glycerol stock solution/water. For this purpose, the ON/OFF switching time of valves $V_{G/B}$ and V_{H2O} was carried to insert differing amounts of the glycerol stock solution and water into FBC, and the stirrer is switched ON during 4 min. Once the standard working solution is prepared into FBC and the stirrer is stopped, the emitter piezoelectric film (PZT_E) is activated for 5 s with a square wave to sonicate and the receiver piezoelectric film (PZT_R) simultaneously translates the acoustic signal received into an electrical signal, which is measured by the data acquisition system. Only the last millisecond is recorded for later analysis. After each measurement, data was downloaded and saved in excel files using the OWON Oscilloscope software. It is worth highlighting that a decrease in signal amplitude with increased concentration of glycerol is observed.

The free glycerol extraction from the biodiesel samples was carried out inside FBC as described by Lima et al. [12]. After, the valve V_{w2} is activated for 10 s to remove the biodiesel phase (BP, Fig. 1). Thereafter, the sample signal is recorded as described just above.

A washing cycle is performed after each measurement. For this purpose, the valve V_{H2O} is switched ON for 15.2 s adding water into FBC and stirrer is switched ON for 30 s. After, the content of FBC is emptied by switching ON valve V_{W2} for 20 s. The washing process was always performed by triplicate.

2.4. Reference method

The chromatographic procedure was carried out according to the reference method (D6584-07 Standard Test Method for the Determination of Free and Total Glycerin in B100 Biodiesel Methyl Esters by Gas Chromatography) [29]. A gas chromatograph, (Agilent Technologies 6890GC) with a flame ionization detector (FID), a programmed temperature vaporizing (PTV) inlet (CIS4, GERSTEL), Dual Rail MPS 2 robotic sampler with 10 mL on-column syringe, and an 80 mL side port syringe with a diluter module (GERSTEL) were used. An Rtx-Biodiesel TG Restek column (10 m × 0.32 mm i.d.) was also used. Each sample solution was injected in triplicate, with a free glycerol retention time of 4.1 min, and the concentrations were calculated from a calibration curve.

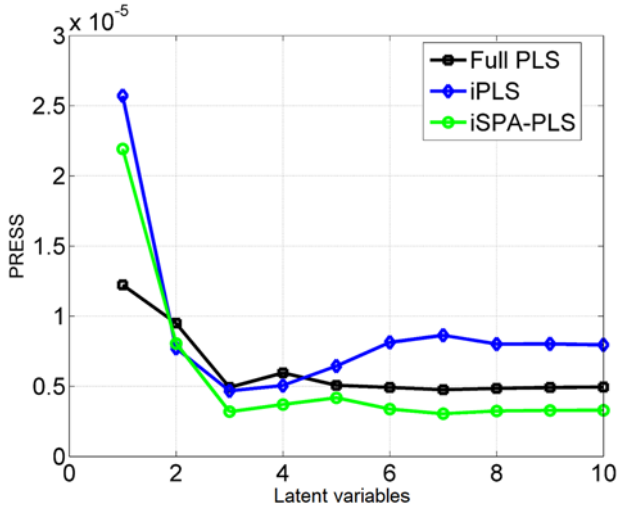

Fig. 4. Press versus variable latents curves for PLS models built using cross validation.

2.5. Chemometrics procedures

Models based on PLS regression were chosen in this work because it is a powerful tool in the construction of multivariate models. Its approach in latent variables makes models less sensitive to instrumental noise. In addition, there was investigated the benefits of discard non-informative variables by means of interval PLS (iPLS) and iSPA-PLS. All PLS models were performed in MatLab using MCV1 [30] and iPLSToolbox [31], both in graphical interface version, available at http://www.iquir-conicet.gov.ar/esp/div5.php?area=12 and http://www.models.kvl.dk/algorithms, respectively. The *i*SPA-PLS calculation was performed by using a routine in command line form.

3. Results and discussions

3.1. Adjustment of the system parameters

By setting the rotation speed of the stirrer at 200 rpm (changing PWM magnitude), the system does not need time for phase separation and emulsion is avoided, as it was done by Lima et al. [12].

In order to obtain reproducible and more sensitive signals, a frequency sweep in the range of 200 Hz to 100 KHz was performed. It was observed that the best sensitivity at changes in low concentrations of glycerol was achieved with a square wave at low frequencies. However, best reproducibility was achieved with a frequency of 1 KHz.

The oscilloscope recorded 5000 values of voltage during 1 millisecond of each received signal (all measurements were made with the same emitted signal). Since the signal was noisy, the raw data was smoothed using the Savitzky-Golay filter with a window of 33 points and a second-order polynomial to remove the systematic noise. Fig. 3 shows curves from the emitted signal applied to the emitter piezoelectric (blue) and the pre-processed received signal of different concentrations of glycerol in water solution (calibration solutions).

Table 2
Statistical summary of fitness and prediction for all PLS models.

Model*	PLS	*i*PLS	*i*SPA-PLS
RMSEC(mg/Kg)	0.419	0.354	0.346
RDP	6.15	7.27	7.44
R^2	0.978	0.959	0.985
Reference value (sd) for test set	Predicted value (sd) for test set		
	PLS	*i*PLS	*i*SPA-PLS
5.9 (0.1)	6.3 (0.1)	5.8 (0.1)	5.9 (0.1)
6.1 (0.1)	6.5 (0.2)	5.3(0.4)	5.8 (0.2)
7.5 (0.2)	7.9 (0.2)	7.1(0.3)	7.4 (0.2)
4.8 (0.1)	5.3 (0.1)	4.4 (0.2)	5.0 (0.1)
7.5 (0.1)	7.8 (0.1)	7.5 (0.2)	7.9 (0.1)
11.8 (0.2)	12.4 (0.4)	12.5 (0.3)	11.9 (0.4)
8.5 (0.2)	9.2 (0.3)	7.9 (0.4)	8.4 (0.3)
REMSP (mg/Kg)	0.498	0.522	0.210
REP (%)	6.57	7.01	2.82
RDP	4.58	4.37	10.87
R^2	0.946	0.981	0.991
γ^{-1} (mg/Kg)	0.021	0.119	0.36
LODmin/LODmax (mg/Kg)	0.64/0.95	0.59/0.89	0.54/0.79
LOQmin/LOQmax (mg/Kg)	1.94/2.84	1.77/2.67	1.62/2.38

Root Mean Square Error Prediction: $RMSEP := \sqrt{\sum_{i=1}^{Npred} \frac{(y_i - \hat{y}_i)}{Npred}}$ *yi* concentration of i^{th} prediction samples determined by reference method, $\hat{y}_i$ concentration of i^{th} prediction samples accessed by PLS model and *Npred* is a quantity of samples from the prediction set.
Relative Error Prediction: $REP = \frac{RMSEP}{\frac{1}{Ncal}\sum_{i=1}^{Ncal} y_{cal\ i}} x\ 100.$
LOD (limit of detection), LOQ (limit of quantitation) and γ-1 (Analytical sensitivity) were estimated based on Net analytical signal approach
RPD (Ratio of Performance to Deviation). RPD = Sd/RMSE; Sd = Standard deviation of the sample.
* All PLS models built using 3 latent variables

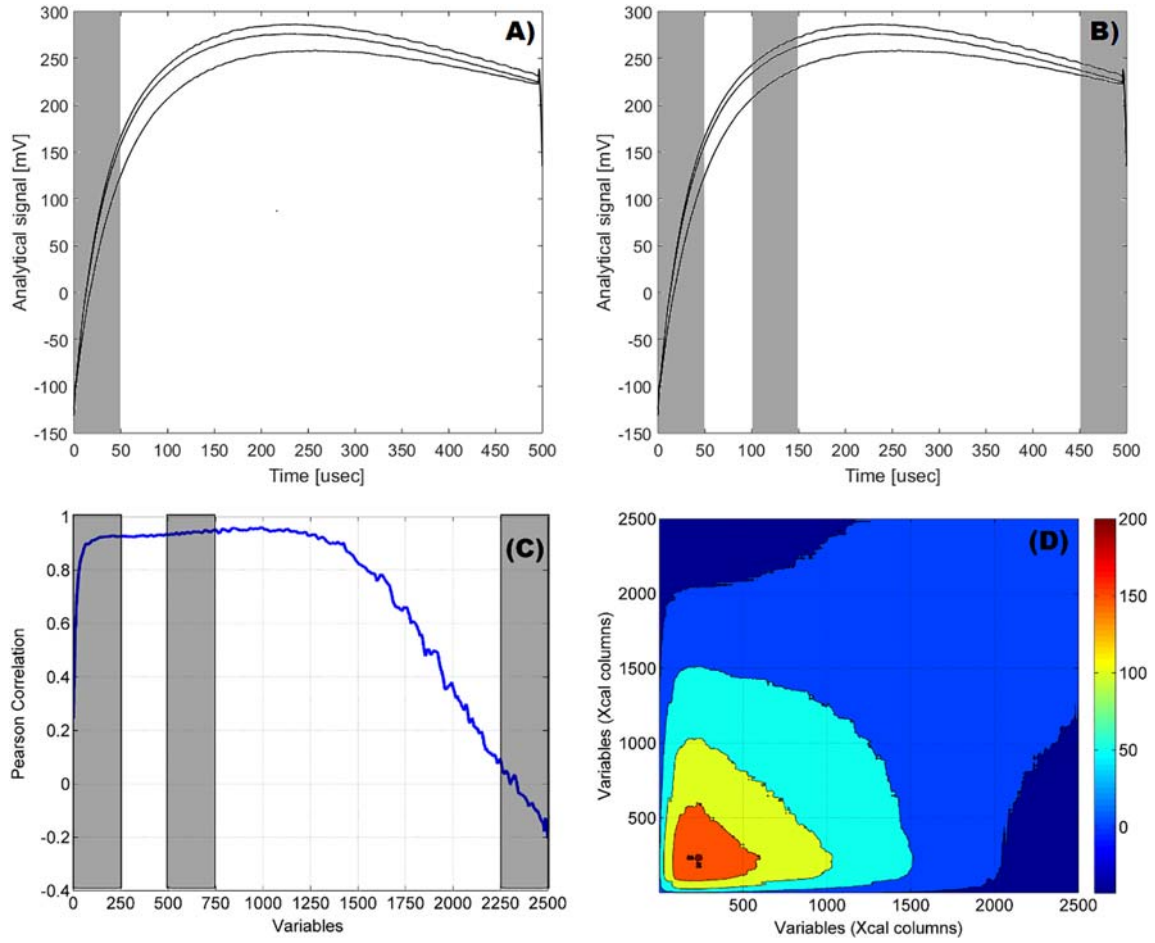

Fig. 5. Selected intervals by iPLS (A) and iSPA-PLS (B) models. Person correlation coefficient of each variable with respect free glycerol content for calibration set (C). Contour surface for covariance of the calibration data (D).

3.2. Interferences

A study of possible piezoelectric-caused temperature variations in the standard solutions and samples was carried out. As the sonication time is short (5 s), and the frequency and amplitude applied to the piezoelectric are low, no significant temperature variation was observed.

After production, the biodiesel is washed exhaustively with water in order to minimize undesirable residues of both reagents and co-products before the commercialization. However, glycerol remains as the major impurity. After extraction, the effects of other possible interferences like alcohols (methanol or ethanol), monoglycerides and diglycerides are negligible. The selectivity of the proposed method was confirmed by GC comparing the shape and the retention time of biodiesel samples with the chromatograms of standard solutions, and no peaks other than glycerol were observed.

3.3. Data set and determination of free glycerol in real samples

The multivariate data recorded in the flow-batch piezoelectric film sensor system was arranged in two matrix arrays; $\mathbf{X_{cal}}_{(18\times2500)}$ and

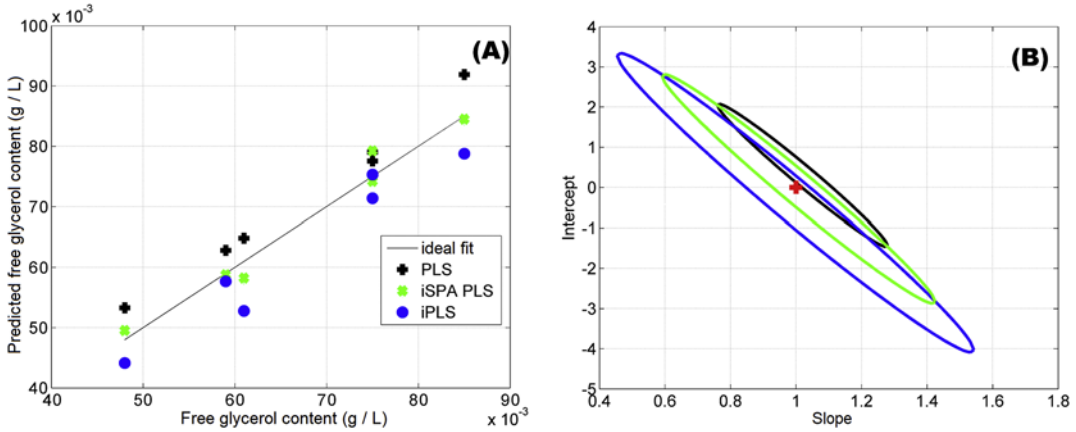

Fig. 6. Predicted versus reference values (A) and elliptical joint confidence regions (B) for PLS models.

Table 3
Comparative features of different methods for determination of free glycerol in biodiesel.

	FIA [10]	MCFA [11]	Batch [13]	FBF [12]	FBS [14]	Proposed
Detection limit [mg kg^{-1}]	5.0	2.0	2.0	0.144	4.0×10^{-6}	0.12
Sampling rate (h^{-1})	90	35	4	14	14	8
Reagents	Water, sodium hydroxide	Water, Hydrochloric acid, ammonium acetate, sodium hydroxide, acetyl acetone, sodium periodate	Water, ethanol, acetic acid, ammonium acetate, potassium periodate, acetyl acetone	Water, acetic acid, ammonium acetate, Potassium periodate, acetyl acetone, isooctane	Water	Water
Extraction	Offline	Offline	–	Online	Online	Online
Sample (mg)	250	1000	1000	15.4	15.4	400
Instrumentation	Potentiometer	Spectro fluorometer	Spectro photometer	Spectro fluorometer	Labmade Luminometer	Piezoelectric Sensor

MCFA: Multicommutation in Flow Analysis; **FIA**: Flow-Injection Analysis; **FBF**: Flow-Batch analyzer with Fluorescence Detection; **FBS**: Flow-Batch analyzer with Sonoluminescence Detection.

$\mathbf{X_{pred}}$ $_{(6\times2500)}$, corresponding to the calibration standard solutions and an external set of prediction (biodiesel samples). For the purpose of building of PLS models, $\mathbf{X_{cal}}$ was evaluated by cross-validation leave-one-out in order to select the number of PLS factors (latent variables). For all PLS models (Fig. 4), the minimum point is obtained using three latent variables and this information was confirmed by F test at a 75% confidence level, criterion used by Haaland and Thomas [32].

A full PLS model and PLS models based on intervals selected by means *i*PLS and *i*SPA-PLS approaches were built with three factors. The performance of these models were proved in the quantification of free glycerol in six biodiesel samples. The statistical summary for fit and prediction is displayed in Table 2.

As it can be seen, small values of calibration errors were obtained for all models and high R^2 values. In addition, ratio performance deviation (RPD) reinforces the idea of well-adjusted models. In prediction of an independent test set, the better accuracy was achieved when PLS was coupled with SPA for intervals selection. The relative error prediction (REP) obtained by *i*SPA-PLS model was 57.1% lower when compared to full PLS model. On the other hand, *i*PLS model presented slightly lower accuracy than full PLS model. In all cases, R^2 presented values very close to 1. As discussed elsewhere [33–34], RPD greater than or equal to 5 can be used for quality control. For all cases, RPDs greater than 5 were achieved in the calibration and prediction steps (see Table 2).

In an attempt to justify the best performance obtained by *i*SPA-PLS, the interval selected (see Fig. 5) by each feature selection (*i*PLS and *i*SPA-PLS) were examined taking into account the full PLS model.

Note that the *i*PLS model selects (see Fig. 5A) only the first interval where the analytical signal intensity is more pronounced. However, the PLS model based only on this interval leds to results with lower accuracy compared to the full PLS model. On the other hand, *i*SPA-PLS selects three intervals (first, third and the tenth, see Fig. 5B).

In Fig. 5C the Person correlation coefficient of each variable with respect to free glycerol content for calibration set is displayed. As can be seen, a part of the variables selected by the *i*PLS have low correlation with the free glycerol content. In addition, the correlation between the variables with each other is pronounced, i.e., a lot of redundant information (see Fig. 5d) that presents a contour surface for covariance of the calibration data, obtained like $\mathbf{X}^T\mathbf{X}$. The diagonal elements of X^TX correspond to the variance of each column vector in X, and the values outside the diagonal are the covariance of one variable relative to the other. High covariance values imply redundant information for the model, which may affect the quality of the model to a greater or lesser extent.

Unlike the *i*PLS model, *i*SPA-PLS selects the first interval, but also selects the third (high correlation, see Fig. 5c) and tenth (region with less redundant variables, see Fig. 5d). Therefore, we believe that the improvements in PLS model adjustments are associated to the removal of redundant and non-informative variables.

The performance of the PLS models can still be examined using curves displayed in Fig. 6. In Fig. 6a, predicted free glycerol content is shown as a function of the values obtained by the reference method (used as true free glycerol content). Note that values predicted by *i*SPA-PLS best fits the ideal line (gray line) in agreement with the low REP value found. Not less important, the absence of significant bias (at a 95% confidence level) in the *i*SPA-PLS model can be contemplated in Fig. 6b. Note that elliptical joint confidence regions (EJCR) for *i*SPA-PLS model contains the ideal point for slope (1) and intercept (0).

3.4. Analytical features

Table 3 compares the analytical features of the proposed method with other procedures described in the literature. The proposed approach is an eco-friendly methodology since it only employs an online free glycerol extraction from biodiesel with water, and completely avoids the use of any chemical reagents and external pretreatment of sample whatsoever during the entire analytical process. This method outperforms a previous work [14] as the PMT is not required allowing the construction of a portable system. Not only the proposed system is less expensive to implement and portable, it also eliminates the requirement of counting with a stabilized and high power utility connection. As it is shown in the experimental evaluation, the response of the proposed method is equivalent to those previously presented but with lower costs and demands.

4. Conclusion

The proposed instrument and method to determine free glycerol in biodiesel has several advantages over conventional procedures and the results agreed with those of the reference method (ASTM D6584-07). In the first place, the analyzer allowed the automatic determination of free glycerol in biodiesel without chemicals/external pretreatment. One of the major features of this system is that takes into account some principles of the green chemistry, such as the decrease in reagent consumption, amount of sample, waste volume (environmentally friendly), and lower energy consumption. This leads to simplicity and fast analysis, which are very important characteristics for routine work. In the second place, there is no need for a PMT which is expensive and requires certain electrical conditions that are not usually available for portable instruments. Finally, several PLS models were built relating free glycerol concentration and the recorded multivariate signal. The better accuracy was achieved when PLS was coupled with SPA for intervals selection. The results shown that with simpler and cheaper equipment than previous works, free glycerol presence in biodiesel can be accurately predicted.

Acknowledgment

The authors gratefully acknowledge Universidad Nacional del Sur (PGI 24/Q079) and CONICET (Consejo Nacional de Investigaciones Científicas y Técnicas) (RD5054) for the financial support. M. Pistonesi

is also grateful to CIC (Comisión de Investigaciones Científicas de la Provincia de Buenos Aires) (Res. 813/13). The authors acknowledge the support of CNPq/CONICET (Brazil/Argentina international cooperation grant 490495/2013-3) and CAPES (studentships).

References

[1] Jidon Janaun, Naoko Ellis, Perspectives on biodiesel as a sustainable fuel, Renew. Sust. Energ. Rev. 14 (2010) 1312–1320.
[2] F. Miran, M.W. Mumtaz, H. Mukhtar, M. Danish, Value-added use of residual glycerol from biodiesel production process via the optimized synthesis of alkyd resins, Process Saf. Environ. Prot. 109 (2017) 659–669.
[3] Q.S. He, J. McNutt, J. Yang, Utilization of the residual glycerol from biodiesel production for renewable energy generation, Renew. Sust. Energ. Rev. 71 (2017) 63–76.
[4] L. Wu, C. Cheng, Flow-injection enzymatic analysis for glycerol and triacylglycerol, Anal. Biochem. 346 (2005) 234–240.
[5] S.G. Silva, F.R.P. Rocha, A flow injection procedure based on solenoid micro-pumps for spectrophotometric determination of free glycerol in biodiesel, Talanta 83 (2010) 559–564.
[6] M. Lapuerta, O. Armas, R. Garcia-Contreras, Pollutant emissions from new European driving cycle with ethanol and butanol diesel blends, Energy Fuel 23 (2009) 4343–4354.
[7] ASTMD6751, Standard Specification for Biodiesel Fuel Blend Stock (B100) for Middle Distillate Fuels, ASTM International, http://www.astm.org.
[8] A.N. Dias, M.B.R. Cerqueira, R.R. de Moura, M.H.S. Kurz, R.M. Clementin, M.G.M. D'Oca, E.G. Primel, Optimization of a method for the simultaneous determination of glycerides, free and total glycerol in biodiesel ethyl esters from castor oil using gas chromatography, Fuel 94 (2012) 178–183.
[9] C.P. Prados, D.R. Rezende, L.R. Batista, M.I. Alves, N.R.A. Filho, Simultaneous gas chromatographic analysis of total esters, mono-, di- and triacylglycerides and free and total glycerol in methyl or ethyl biodiesel, Fuel 96 (2012) 476–481.
[10] A.H. Maruta, T.R. Paixão, Flow injection analysis of free glycerol in biodiesel using a copper electrode as an amperometric detector, Fuel 91 (2012) 187–191.
[11] S.G. Silva, Á. Morales-Rubio, M. de La Guardia, F.R.P. Rocha, Sequential spectrofluorimetric determination of free and total glycerol in biodiesel in a multicommuted flow system, Anal. Bioanal. Chem. 401 (2011) 365–371.
[12] M.B. Lima, M. Insausti, C.E. Domini, M.F. Pistonesi, M.C.U. de Araújo, B.S.F. Band, Automatized flow-batch method for fluorescent determination of free glycerol in biodiesel samples using on-line extraction, Talanta 89 (2012) 21–26.
[13] M.S. Ribeiro, F.R. Rocha, A single-phase spectrophotometric procedure for in situ analysis of free glycerol in biodiesel, Microchem. J. 106 (2013) 23–26.
[14] P.H.G.D. Diniz, M.F. Pistonesi, M.C.U. de Araújo, B.S.F. Band, Eco-friendly sonoluminescent determination of free glycerol in biodiesel samples, Talanta 114 (2013) 38–42.
[15] J. Wu, D. Xiao, J. Zhu, Potassium-sodium niobate lead-free piezoelectric materials: past, present, and future of phase boundaries, Chem. Rev. 115 (2015) 2559–2595.
[16] B. Zaitsev, A. Teplykh, I. Borodina, I. Kuznetsova, E. Verona, Gasoline sensor based on piezoelectric lateral electric field excited resonator, Ultrasonics 80 (2017) 96–100.
[17] B. Wang, X. Chu, E. Li, L. Li, Simulations and analysis of a piezoelectric micropump, Ultrasonics 44 (2006) e643–e646 (Proceedings of Ultrasonics International (UI′05) and World Congress on Ultrasonics (WCU)).
[18] T. Ikeda, Fundamentals of Piezoelectric Materials Science, Ohm Publication Company, Tokyo, 1984 83.
[19] H. Kawai, The piezoelectricity of poly (vinylidene fluoride), Jpn. J. Appl. Phys. 8 (1969) 975.
[20] Piezo Film Sensor. Technical Manual, http://emerald.tufts.edu/programs/mma/emid/piezo.pdf.
[21] P. Ueberschlag, PVDF piezoelectric polymer, Sens. Rev. 21 (2001) 118–126.
[22] K.H. Baumgärtel, D. Zöllner, K.-L. Krieger, Classification and simulation method for piezoelectric PVDF sensors, Procedia Technol. 26 (2016) 491–498 (3rd International Conference on System-Integrated Intelligence: New Challenges for Product and Production Engineering).
[23] I. Jung, Y.-H. Shin, S. Kim, J. young Choi, C.-Y. Kang, Flexible piezoelectric polymer-based energy harvesting system for roadway applications, Appl. Energy 197 (2017) 222–229.
[24] A. Spanu, L. Pinna, F. Viola, L. Seminara, M. Valle, A. Bonfiglio, P. Cosseddu, A high-sensitivity tactile sensor based on piezoelectric polymer PVDF coupled to an ultra-low voltage organic transistor, Org. Electron. 36 (2016) 57–60.
[25] Y. Xin, X. Qi, C. Qian, H. Tian, Z. Ling, Z. Jiang, A wearable respiration and pulse monitoring system based on PVDF piezoelectric film, Integr. Ferroelectr. 158 (2014) 43–51.
[26] D. Chen, M. Hang, K. Chen, K. Brown, J.X.J. Zhang, Piezoelectric PVDF 19 thin films with asymmetric microporous structures for pressure sensing, 2015 IEEE SENSORS 2015, pp. 1–4.
[27] P.H.G.D. Diniz, M.F. Pistonesi, M.C.U. Araujo, Using iSPA-PLS and NIR spectroscopy for the determination of total polyphenols and moisture in commercial tea samples, Anal. Methods 7 (2015) 3379–3384.
[28] A.A. Gomes, R.K.H. Galvão, M.C.U. de Araújo, G. Véras, E.C. da Silva, The successive projections algorithm for interval selection in PLS, Microchem. J. 110 (2013) 202–208.
[29] ASTMD6584-07, Test Method for the Determination of Free and Total Glycerin in B100 Biodiesel Methyl Esters by Gas Chromatography, ASTM International, http://www.gerstel.com.
[30] MVC1: programa para calibración multivariada de primer orden en MATLAB, http://www.iquir-conicet.gov.ar/esp/div5.php?area=12.
[31] iPLSToolbox, http://www.models.kvl.dk/algorithms.
[32] D.M. Haaland, E.V. Thomas, Partial least-squares methods for spectral analyses. 1. Relation to other quantitative calibration methods and the extraction of qualitative information, Anal. Chem. 60 (1988) 1193–1202.
[33] C.W. Chang, D.A. Laird, M.J. Mausbach, C.R. Hurburgh, Near-infrared reflectance spectroscopy - principal components regression analyses of soil properties, Soil Sci. Soc. Am. J. 65 (2001) 480–490.
[34] P.C. Williams, Variables affecting near-infrared reflectance spectroscopic analysis, in: P. Williams, K. Norris (Eds.), NearInfrared Technology in the Agricultural and Food Industries, American Association of Cereal Chemists Inc., Minnesota 1987, pp. 143–167.